Atmos. Chem. Phys. Discuss., 8, 16061–16096, 2008
www.atmos-chem-phys-discuss.net/8/16061/2008/

Atmospheric Chemistry and Physics Discussions

This discussion paper is/has been under review for the journal *Atmospheric Chemistry and Physics (ACP)*. Please refer to the corresponding final paper in *ACP* if available.

Saharan dust transport and deposition towards the Tropical Northern Atlantic

K. Schepanski[1,2], I. Tegen[1], and A. Macke[2]

[1]Leibniz Institute for Tropospheric Research, Leipzig, Germany
[2]Leibniz-Institute of Marine Sciences, IFM-GEOMAR, Kiel, Germany

Received: 17 June 2008 – Accepted: 1 July 2008 – Published: 22 August 2008

Correspondence to: K. Schepanski (kerstin.schepanski@tropos.de)

Published by Copernicus Publications on behalf of the European Geosciences Union.

Abstract

We present a study of Saharan dust export towards the tropical North Atlantic using the regional dust emission, transport and deposition model LM-MUSCAT. Horizontal and vertical distribution of dust optical thickness, concentration, and dry and wet deposition rates are used to describe seasonality of dust export and deposition towards the eastern Atlantic for three exemplary months in different seasons. Deposition rates strongly depend on the vertical dust distribution, which differs with seasons. Furthermore the contribution of dust originating from the Bodélé Depression to Saharan dust over the Atlantic is investigated. A maximum contribution of Bodélé dust transported towards the Cape Verde Islands is evident in winter when the Bodélé source area is most active and dominant with regard activation frequency and dust emission. Limitations of using satellite retrievals to estimate dust deposition are highlighted.

1 Introduction

The Sahara as the World's most important dust source adjoins directly to the Atlantic ocean (e.g. Prospero et al., 2002; Middleton and Goudie, 2001; Goudie and Middleton, 2001; Washington et al., 2003). A major part of the Saharan mineral dust is exported towards the northern tropical Atlantic (e.g. Romero et al., 1999). Mineral dust consists of small soil particles with regionally specific mineralogical, chemical, physical, and optical properties. Besides the interactions with solar and thermal radiation as well as clouds during transport, mineral dust deposited onto soil or ocean surfaces acts as nutrient for terrestrial and oceanic ecosystems (e.g. Mahowald et al., 2005). The bio-availability of micro-nutrients in mineral dust particles depends on their mineralogical and chemical properties that depend on source area mineralogy, and processes on the particle surfaces during transport in dry or aqueous phases (Goudie and Middleton, 2001; Luo et al., 2003; Journet et al., 2008). The Earth's surface contain around 4% of iron (Wedepohl, 1995) and consequently soil-derived mineral dust can be considered as transport medium for iron from soil surface into ocean regions (Fung et al., 2000; Sarthou et al., 2003; Jickells et al., 2005). Iron in its role as micro-nutrient for ocean-ecosystems acts as controlling factor for life in high-nitrate, low chlorophyll (HNLC) regions, e.g. for phytoplankton growth (Neuer et al., 2004; Mahowald et al., 2005; Moore et al., 2006; Sarthou et al., 2007). In the tropical Atlantic, iron delivered by dust particles may enhance nitrogen fixation. By these processes dust deposition may be coupled to the CO_2 budget and climate system (Gao et al., 2001 and references therein). Remote sensing retrievals have been used to determine dust fluxes into the North Atlantic, assuming that the ratio of atmospheric dust load within a column and the corresponding aerosol optical thickness (AOT) can be described by a fixed value (e.g. Kaufman et al., 2005). Based on such analyses of satellite retrievals, the Bodélé Depression was claimed to be the major source for dust transport to the Amazon (Koren et al., 2006). Oceanic dust deposition has also been estimated from global dust models (e.g. Zender and Newman, 2003; Mahowald et al., 2005). Regional models are suitable to investigate dust conditions for specific meteorological situations and are expected to provide better vertical resolution of dust layers compared to global-scale models, which is an important control of dust deposition. This paper aims to show exemplarily for three single case studies the characteristics as well as the differences of dust transport concerning e.g. direction, height, and amount, and dust deposition towards the eastern tropical North Atlantic in different seasons. The contribution of dust emitted over the Bodélé Depression to the total exported Saharan dust will be determined. Furthermore the relation of aerosol optical thickness (AOT) of dust (in the following refereed as AOT) and atmospheric dust column load and deposition fluxes is discussed. This aims at the question whether it is possible to derive dust deposition from AOTs based on measurements of space borne instruments like e.g. MODIS or SeaWiFS.

2 Regional model system LM-MUSCAT

To characterise Saharan dust transport and deposition towards the tropical North Atlantic, we use the dust transport model system LM-MUSCAT (Heinold et al., 2007). It consists of the regional scale meteorological model LM (provided by the Deutscher Wetterdienst, Doms and Schättler, 2002) and the MUlti-Scale Chemical Aerosol Transport Model (MUSCAT, Wolke et al., 2004a; Wolke et al., 2004b). The dust transport model includes a dust emission scheme based on Tegen et al. (2002). Meteorological and hydrological fields used for the simulation of dust emission, transport and deposition, are computed by the LM and updated in MUSCAT at every advection time step of 80 s. Local wind systems, clouds, precipitation, and meso-scale convection depend on topography. For simulation of sub-grid scale moist convection the parameterisation following Tiedtke (1989) is used in the LM. Dust emission is modified by surface properties like vegetation, surface roughness, soil texture and soil moisture content. In addition to soil properties, wind shear stress at the ground is the major limiting factor for soil erosion. The wind shear stress τ is related to the air density ρ_a and the friction velocity u_*, following $\tau=\rho_a u_*^2$. Dust emission occurs if the friction velocity exceeds a local, soil-dependent threshold u_{*t} for dust mobilisation. Here a parameterisation for u_{*t} based on Iversen and White (1982) is used, modified by Marticorena and Bergametti (1995). Airborne dust is transported as passive tracer in five independent size bins (radius limits at: 0.1 μm, 0.3 μm, 0.9 μm, 2.6 μm, 8 μm and 24 μm). For each size bin spherical dust particles following a log-normal size distribution are assumed. Dust deposition is parameterised as dry and wet deposition. The parameterisation of dry deposition depends on particle size, density and meteorological conditions affecting the behaviour of dust particles. In detail the parameterisation considers turbulent transfer, Brownian diffusion, impaction, interception, gravitational settling, and particle rebound. Dry deposition of the dust is controlled mainly by gravitational settling, which is dominant for particles larger than 2 μm, and the impact of aerodynamic (R_a) and surface resistance (R_s). Gravitational settling, commonly described by the gravitational settling velocity v_d is based on the Stoke's equation describing the equilibrium of gravitation and buoyancy:

$$v_g = \frac{(\rho_p - \rho_a) g D_p^2 C_c}{18\eta} \tag{1}$$

with particle diameter D_p, air density ρ_a, particle density ρ_p=2.65 g/cm^3, the gravitational constant g, the dynamic viscosity of air η, and the Cunningham correction factor C_c. The Cunningham correction takes into account that the Stoke's law considers the velocity of the air surrounding the particle's surface relative to the particle itself as zero. This assumption is correct in continuum but not for particle larger than the mean free path λ of air molecules. The Cunningham correction factor C_c is used to take this into account and is described by

$$C_c = 1 + \frac{2\lambda}{D_p}\left[1.142 + 0.558 \exp\left(-\frac{0.4995 D_p}{\lambda}\right)\right]. \tag{2}$$

For particles smaller than 2 μm, the gravitational settling velocity v_g is adjusted by the aerodynamic and surface resistance R_a and R_s:

$$v_d = \frac{1}{R_a + R_s + R_a R_s v_g} + v_g. \tag{3}$$

Beside dry deposition, especially over the North Atlantic, wet deposition, e.g. by rainout, has an increasing influence on particle removal. In MUSCAT, the parameterisation follows e.g. Berge (1997), Jacobson et al. (1997) and bases on the parameterisation used in the EMEP MSC-W Eulerian model by Tsyro and Erdman (2000). Wet deposition is controlled by the precipitation rate p and the scavenging coefficient λ,

$$\text{Dep\_rate} = -\lambda \cdot p, \tag{4}$$

with

$$\lambda = \frac{A \cdot E}{v_{dr}}, \tag{5}$$

ACPD

8, 16061–16096, 2008

Seasonal Saharan dust transport and deposition

K. Schepanski et al.

related to an empirical coefficient A=5.2 m^3/kg s due to Marshall-Palmer size distribution assumed for rain drops, to the mean collection efficiency E, averaged over all rain drop sizes and to the rain drop fall velocity v_{dr}, here v_{dr}=5 m/s. For the computation of AOT at 550 nm, dust concentrations of the five size bins (dust mode, j) are used. The dust particles are assumed to be spherical particles with a density of quartz (ρ=2.65 g/cm^3):

$$\tau = \sum_j \sum_k \left(\frac{3}{4} \frac{Q_{\text{ext},550}(j)}{r_{\text{eff}}(j)\rho_p(j)} c_{\text{dust}}(j,k)\Delta z(k) \right), \tag{6}$$

with the extinction efficiency $Q_{\text{ext},550}(j)$ (derived from Mie-theory), effective radius of dust particle $r_{\text{eff}}(j)$, dust concentration $c_{\text{dust}}(j,k)$ at vertical level k, and the vertical increment of each vertical level $\Delta z(k)$. For this study of dust transport and deposition towards the tropical North Atlantic, we run the model system on a 28 km horizontal grid resolution and 40$\sigma-p$ levels up to 12 km height. The first level is centred around 38 m above ground level (agl). There is a spin-up period of 24 h for the LM part, after this period the MUSCAT is coupled to the LM. Every 6 h, meteorological boundary conditions are updated with analysis fields from GME (global weather forecast model of the DWD). After 24 h of LM-MUSCAT computations, the meteorological fields are reinitialised. Three case studies of one month periods, in different seasons have been computed: March 2006, July 2006 and 20 December 2006 to 20 January 2007 (hereafter refereed as January 2007).

3 Dust transport and deposition towards the tropical North Atlantic

The Sahara and Sahel region over North Africa contains several potential dust source areas, mostly located in the foothills of the mountain areas where endoheric drainage systems and wadis opening to fluvial fans provide a large amount of sediment available for aeolian erosion (e.g. Washington et al., 2003; Schepanski et al., 2007). Each dust source area is characterised by seasonal and annual changes in frequency of dust source activation (Schepanski et al., 2008[1]). Consequently, seasonal changes in spatio-temporal dust source activity are related to seasonal changes in local meteorological conditions providing atmospheric conditions for dust mobilisation. However, as local meteorological conditions are influenced by regional and meso-scale meteorological systems, dust transport is affected regarding amount, height of transport layer, and dry and wet deposition rates respectively. To investigate exemplary transport and deposition patterns of Saharan dust in different seasons, three modelling studies for one month periods (March 2006, July 2006 and January 2007) representing different seasons (north hemispheric spring, summer and winter) have been preformed using regional model system LM-MUSCAT.

3.1 Characteristics of Saharan dust transport

To describe the horizontal distribution of atmospheric dust load, we must distinguish between near-source area, areas affected by dust transport over the African continent and over the ocean. The atmospheric dust concentration over the near source area is mainly characterised by the dust source activity, the wind direction and speed, and the buoyancy (Kalu, 1979). The dust particle sizes are larger close to the source region and decrease with distance due to gravitationally settling. Dust is mixed up by turbulent mixing within the boundary layer (BL), transported within the regional wind flow or washed out by rain-events. During transport, the dust plume can remain near the surface and be observed as dust storm, or can be transported as elevated layer. Within the BL, dust concentration can be homogeneously distributed over the entire BL depth (Tesche et al., 2008[2]). In the evening, mixing activity within the BL ceases

[1] Schepanski, K., Tegen, I., Todd, M. C., Heinold, B., Bönisch, G., Laurent, B., and Macke, A.: Meteorological processes forcing Saharan dust emission inferred from MSG-SEVIRI observations of sub-daily dust source activation, J. Geophys. Res., submitted, 2008.

[2] Tesche, M., Ansmann, A., Müller, D., Althausen, D., Mattis, I., Heese, B., Freudenthaler, V., Wiegner, M., Esselborn, M., Pisani, G., and Knippertz, P.: Vertical profiling of Saharan dust

and a significantly shallower nocturnal BL remains (Garratt, 1992). However, airborne dust can be still present in the residual layer. This decoupled air layer can be seen as a elevated air layer. During night, the air layer remain stationary and will be re-mixed to the developing daytime BL (Blackadar, 1957; Lenschow and Stankov, 1979; Kalu, 1979). Alternatively, geostrophic forces may lead to acceleration of the air mass above the nocturnal BL up to super-geosptrophic wind speeds, a nocturnal low-level jet (LLJ) develops (e.g. Nappo, 1991; Banta et al., 2006; Schepanski et al., 2008[1]) and the elevated air mass with its dust content is transported away from the source area (Kalu, 1979). Transported dust layers during night within a LLJ might be mixed into the developing BL the next day. Decreasing horizontal visibilities have been observed during the build-up phase of the daytime BL (Kalu, 1979). Atmospheric dust layers that are transported away from the sources can be elevated to higher levels compared to source areas. The elevation of dust layers depends on the season (see Fig. 1). During winter, the dust layers over the West African continent are situated at lower levels than during summer (Kalu, 1979). In winter months, transported Saharan dust is observed and reproduced by regional model studies near the surface, while in summer the dust layer is elevated. This is due to seasonal different meteorological regimes especially over the Sahel and the Western Sahara. Due to northward shift of the ITD (inner-tropical discontinuity, marking the meeting of dusty desert air and tropical moist air) the BL is deeper during summer which results in a higher upward-mixing of dust. During night the West African Monsoon (WAM) circulation forces the development of high geostrophic wind speeds in the decoupled, elevated air layer (e.g. Parker et al., 2005). Dust can be mixed up high into troposphere and be transported fast during night. Additional, dust layers within the mid-troposphere overlay the moist and denser monsoon air and reaches higher transport levels in summer than in winter when the dust layer is transported within the trade winds (Kalu, 1979). The location of the ITD is father south in winter, so the high vertical mixing of dusty air occurs further south

with Raman lidars and airborne HSRL in southern Morocco during SAMUM, Tellus, revised, 2008.

over the South Sahel/Savanna. In summer this strong mixing occurs further north over the Sahel/South Sahara due to northward shift of the Hadley circulation (see also Fig. 2a and c). Over the ocean, the Saharan dust layer is transported above the trade winds inversion (up to 5–7 km above sea level) (Kalu, 1979; Chiapello et al., 1997; Dunion and Velden, 2004) in north hemispheric summer (Fig. 1). In winter the dust is transported within the trade wind layer at altitudes below 1.5–3 km (Chiapello et al., 1997, Barkan et al., 2004). Horizontal dust transport paths can be tracked considering the horizontal AOT distribution. Figure 2 shows the monthly mean AOT computed from LM-MUSCAT results and MODIS retrievals for North Africa and the tropical East Atlantic for January 2007 (a), March 2006 (b) and July 2006 (c), exemplarily for different seasons. As AOT retrievals from remote sensing data are difficult for areas with bright surfaces, no AOT retrievals are available over the desert. In winter (January 2007, Fig. 2a), the mean AOT is highest over the Sahel and Savanna. AOT over the Sahara and Maghreb (Morocco, Algeria, Tunisia, Libya) is very low (less than 0.1) pointing towards high dust source activity in the southern Sahara and Sahel and less in the northern part. The Bodélé as a dust source with most frequent dust source activity during winter (Schepanski et al., 2008[1]) is well marked by high mean AOT (1.6). In spring (March 2006, Fig. 2b), the pattern of the mean AOT distribution is nearly the same as in winter, but the mean values are higher. These differences can be explained by different dust source characteristics. In spring, additional to the Bodélé source area, dust sources in the foothills around the Hoggar-Adrar-Air Massif are more active than in winter. The same is the case for the Akhdra Mountains in Tunisia (mean AOT up to 0.7). Furthermore, in March 2006 an extreme dust event occurs, activated in the Atlas Mountains by a crossing upper-level trough triggering a meso-scale density current (Knippertz et al., 2008[3]). This extraordinarily strong dust plume significantly

[3]Knippertz, P., Ansmann, A., Althausen, D., Müller, D., Tesche, M., Bierwirth, E., Dinter, T., Müller, T., von Hoyningen-Huene, W., Schepanski, K., Wendisch, M., Heinold, B., Kandler, K., Petzold, A., Schütz, L., and Tegen, I.: Dust Mobilization and Transport in the Northern Sahara during SAMUM 2006 – A Meteorological Overview, Tellus, revised, 2008.

influences the mean AOT, especially over Algeria, where local maxima of up to 0.6 occur, while in the vicinity mean AOT values of 0.3 are present. Areas where dust remains in the atmosphere have higher mean AOT values than dust source areas with less frequent activity. The Savanna and the local maxima areas over the coastal region characterised by high mean AOT values are not strong dust sources, but are strongly influenced by dust transport in southerly direction. The dusty air originating from the Sahara and Sahel meets tropical air masses marking the ITD. There the dusty air mass is mixed up while remaining more or less stationary, leading to high mean AOT values. This characteristic can also be observed with the MSG IR dust index. In summer, the maximum mean AOT occurs over central Mali. During this season, the region is influenced by the Saharan heat low and air circulation is forced by the WAM. This circulation forces dust source activation during the morning hours (Schepanski et al., 2008[1]) due to down-mixing of momentum related to nocturnal LLJs. Furthermore the WAM is characterised by a strong vertical mixing so that airborne dust can be efficiently mixed up into higher tropospheric levels.

Dust transport direction is strongly dependent on the leading wind regime. The mean AOT distribution indicates a strong westward transport during summer and a southwest transport during winter, mainly affected by the location of the subtropical high pressure system and the ITCZ (inner-tropical convergence zone, Prospero et al., 1981; Chiapello et al., 1995; Chiapello et al., 1997). Both, AOT computed from modelling results and MODIS measurements, show similar seasonal pattern. Nevertheless, MODIS AOT values are lower than modelled ones. The AOT differences may be partly caused by the lower temporal resolution of measurements compared to hourly extracted modelled AOT values. However, stationary dust clouds cause high mean AOT values. Furthermore, clouds inhibit AOT retrievals from satellite measurements. In July 2006, both, AOT computed from model results and MODIS retrievals show lower AOTs than in winter. Modelled AOT is lower over the ocean than the values from MODIS measurements and the AOT pattern matches less well than in other seasons. As in the summer months dust emission over Western Africa is frequently triggered by moist convection events, the lower modelled AOT is presumably related to shortcomings of modelling moist convection in the LM (Heinold et al., 2008)[4].

3.2 Monthly distribution of dry and wet dust deposition

Airborne dust can be removed from the atmosphere by dry or wet deposition. The relative importance of dry or wet deposition processes differs regionally and changes with seasons (Fig. 3). During winter (January 2007, Fig. 3a), wet deposition is negligible over nearly the entire North African domain, while dry deposition is very dominant and represents the pattern of mean AOT. High dry deposition rates over Tunisia, the western foothills of the Hoggar Massif and western Algeria in the presence of relative low mean AOT values (Fig. 2) indicate near-source deposition and short residence time of dust within the atmosphere. Wet deposition occurs mainly over the Atlantic related to moist convection within the tropical convergence zone and low pressure disturbances further north. Over the tropical East Atlantic, the Saharan Air layer (SAL), a very dry, warm and dusty air mass originating from the desert, is characterised by negligible wet deposition (lower than 0.01 g/m^2), high dry deposition (up to 1 g/m^2) rates compared to other Atlantic regions and high mean AOT (Figs. 2 and 3). During March 2006 (not shown) representing a spring month, the same features as described for January 2007 can be found. The domain of high dry deposition rates and negligible wet deposition rates is centred further north due to northward shift of Hadley circulation. In summer, moist convection occurs especially over the mountains and the monsoon region. Thus wet deposition occurs especially over the West Sahara, the Sahel and the Atlas Mountains. Dominance of wet deposition is indicated by high deposition rates (up to 10 g/m^2 over the Atlas and up to 5 g/m^2 over the West Sahara) in these areas. High dry deposition rates are also found over the West and Central Sahara (up to 10 g/m^2). The

[4]Heinold, B., , Tegen, I., Esselborn, M., Kandler, K., Knippertz, P., Müller, D., Schladitz, A., Tesche, M., Weinzierl, B., Ansmann, A., Althausen, D., Laurent, B., Petzhold, A., and Schepanski, K.: Regional Saharan Dust Modelling during the SAMUM 2006 Campaign, Tellus, revised, 2008.

coincidence of both, dry and wet deposition in this region are a main characteristic of summer months and point towards the unsettled weather character of the monsoon period.

3.3 Temporal evolution of the dust concentration over the Cape Verde Archipelago

The Cape Verde Islands, located 460 km west offshore the West African coast in the tropical Atlantic are a suitable location to study Saharan dust transport and deposition. Dust transported towards the Cape Verde is variable in time as it depends on the spatiotemporal distribution of dust source activities, on transport paths affected by wind direction and speed, and deposition and scavenging processes during transport. Furthermore, the Cape Verde Archipelago is in the focus of several field studies like SAMUM-II (SAharaN Mineral dUst experiMent, http://samum.tropos.de), SOPRAN (Surface Ocean Processes in the Anthropocene, http://sopran.pangaea.de) and SOLAS (Surface Ocean Lower Atmosphere Study, http://www.solas-int.org) as well as location of the Tropical Eastern North Atlantic Time-Series Observatory TENATSO (http://tenatso.ifm-geomar.de) and an AERONET (AErosol RObotic NETwork, http://aeronet.gsfc.nasa.gov) station. Figure 4 shows the temporal evolution of AOT over Sal, Cape Verde for the modelling results and AERONET sun-photometer measurements. Comparing AOT computed from LM-MUSCAT model results to the sun-photometer measurements, main features of the passing dust plumes represented by individual peaks are well reproduced. Beside capturing the temporal evolution of transported dust, the magnitude of AOT is well reproduced by the model, especially in January 2007 and in the beginning of March 2006. After 10 March the model overestimates the observations by about a factor of 2. In July, the model results do not capture the temporal evolution of AOT well but the magnitude of AOT is well reproduced by the model at this location, even though deviations exist in the comparison with MODIS AOT retrievals (see above). Comparison with deposition fluxes (Fig. 4) indicate that discrepancies between modelled and observed AOT may be due to too efficient wet deposition in this month. Shortcomings in temporal evolution might be due to less accurate reproduction of moist convection in the source region. The temporal evolution of AOT maxima indicate individual dust plumes transported towards the Cape Verde Islands. The AOT as a measure for total dust concentration within the atmospheric column above the reference point does not give any information about the vertical distribution of the dust concentration. The regional model LM-MUSCAT provides information about the vertical dust distribution in addition to the column load or AOT. Figure 5 shows the modelled temporal evolution of vertical dust concentration over the Cape Verde at 16° N; 22° W for January 2007 and March and July 2006 representing the characteristics of the different seasons. During winter, the dust transport layer is situated at lower tropospheric levels with maximum dust concentrations up to around 2 km on most days. Frequently the dust layer extends down to (near-)surface layers (Fig. 5). In summer, the dust transport layer is the Saharan Air Layer (SAL), which is aloft in heights around 4–5 km and does not extend to the ground levels (see also Sect. 3.1 and Fig. 5c). During spring, the dust transport layer can be found in lower tropospheric layers (up to around 2 km) as well as in higher levels (around 4 km height). Dust transport in spring is characterised by a transition from lower (winter) transport heights to high (summer) transport heights (Fig. 5b). Comparing both the AOT (Fig. 4) and vertical dust concentration distributions (Fig. 5), it is obvious that high AOT do not necessarily indicate high surface dust concentrations. However, high dust concentrations at surface levels are coincident with high deposition rates (Figs. 4 and 5). The relation between these three measures are strongly impacted by the height of the dust layer. In winter when the dust layer is situated within the lower troposphere or near the surface within the trade wind layer, high dust deposition rates coincide with high dust concentrations and high AOT values. In summer, this coincidence is not evident due to the dust transport occurring in an elevated layer above the trade winds inversion. However, the dust deposition at a specific location is not closely linked to the AOT (Fig. 4). Dust deposition depends rather on the vertical distribution of dust concentrations for which the AOT does not take account.

3.4 Zonal dust flux

Besides the horizontal distribution of AOT, dust concentration and dust deposition, zonal dust fluxes can be used to describe dust transport. In case of the Saharan dust export towards the North Atlantic, zonal fluxes can be used to estimate Saharan dust export due to the dominant zonal wind direction in all seasons (e.g. Kaufman et al., 2005). Here we computed monthly zonal dust fluxes at 10° W, 15° W and 20° W (Fig. 6) using the results from the regional dust emission and transport model. Zonal dust fluxes F_{dust} are calculated using zonal wind speed u and dust concentration M_{dust}:

$$F_{\text{dust}} = M_{\text{dust}} \cdot u. \tag{7}$$

The 10° W meridian crosses the Western Sahara, so the western-most Saharan dust sources will be missed but dust export tracking over the Gulf of Guinea and the Canary Islands will be captured close to the coast. The 20° W meridian is located over the Atlantic. Both meridional transects start at 2.5° N and end at 40° N, limited by the domain of the regional model LM-MUSCAT. The vertical structure of monthly zonal dust export for winter (January 2007) and summer (July 2006) is shown in Fig. 6. In winter, most of the dust is transported within the lower tropospheric layers, peaking between 12° N and 16° N with a maximum dust export per layer at −1 Mg/month at 10° W (the negative sign indicating westward transport). At 20° W, maximum of dust export is shifted further northward and peaking at around 17° N with a maximum export of −3 Mg/month (see Table 1). Above the layers with strong westward dust export, especially at the 20° W meridian, a significant eastward back-transport of Saharan dust occurs. In the tropics, the Hadley circulation is dominant and provides east to northeasterly surface winds related to the subtropic high-pressure system and the tropical low-pressure zone. In the upper troposphere, low pressure is evident over the subtropical surface high due to descending of air masses and high pressure over the tropical depression due to ascending air. Consequently, in the upper troposphere the air flow is reversed. Once Saharan dust has reached the upper troposphere, it can be transported back from the Atlantic towards Africa. Additionally to a strong westward dust export in the lower troposphere over the tropics, an eastward back-transport is significant over the subtropical Atlantic (around 30° N) at 20° W. During winter extra-tropical cyclogenesis occurs over the subtropical Atlantic leading to transport of dust back to the Sahara. In summer, the zone of maximum dust export from the Sahara is located at higher altitudes due to elevation of dust layer above the monsoon layer and shifted to the north, related to the northward shift of the Hadley circulation. The maximum dust export at one level reaches values of −0.1 Mg/month and −8 Mg/month respectively, see Fig. 6. Furthermore, the dust layer raises at the distance between 10° W and 20° W due to overlaying the moist marine air masses. While in winter the southeast part of the Sahara is a more active dust source area, in summer the western part is the more active source region (Schepanski et al., 2008[1]). In winter, caused by location of active source area and south to southwesterly transport direction (into the Sahel and Savanna sector), most of the dust is exported towards the Atlantic at tropical latitudes. In summer, the Western Sahara is the most active part and, additionally, westerly winds transport the Saharan dust towards the Atlantic. At tropical latitudes the monsoon circulations forced by the Saharan heat low transports dust back towards the African continent. As described above, in the upper troposphere the wind direction is reversed which is also evident in summer at both longitudinal transects. The dust export towards the North Atlantic computed by the regional model LM-MUSCAT show clearly the seasonal shift in wind regimes influencing the dust transport in the lower and in the upper troposphere.

3.5 Bodélé dust

The Bodélé Depression is the single most active dust source area of the world (e.g. Prospero et al., 2002) and is characterised by a maximum activity in winter and minimum during summer months (Schepanski et al., 2008[1]). The Bodélé, now located a hyper-arid zone, was a fresh-water lake about 6 000 years ago (Lake Mega-Chad, Washington et al., 2003). Today, a hard crust of diatomite covers the former lake floor and provides a large amount of dust by aeolian erosion Washington et al. (2003). It has been claimed that the diatomite-rich dust originating from the Bodélé Depression has an important fertilising impact on the Amazonian rain forest in South America (e.g. Koren et al., 2006). Here we use the regional model LM-MUSCAT to evaluate the fraction of Bodélé dust over North Africa and the adjacent East Atlantic (Figs. 7 and 8). Due to changing source activity with the seasons, the contribution of Bodélé dust to the total dust load and deposition changes with seasons as well. During winter, the Bodélé Depression is the most active source over the entire Sahara and Sahel domain (Schepanski et al., 2008[1]) and consequently the contribution of Bodélé dust is highest during this season. The present modelling study show a part of Bodélé from up to 50% over the Cape Verde Archipelago. During summer, when the dust source activity in the Bodélé Depression reaches minimum (Washington and Todd, 2005; Schepanski et al., 2008[1]), its contribution to the atmospheric dust content is low (up to 14% over the Cape Verde Islands). Beside the low source activity in the Bodélé, other source areas show a high activation frequency and are dominant (Schepanski et al., 2008[1]). Over the northern Sahara and the extra-tropical Atlantic, the contribution of dust originating from the Bodélé is significantly lower than over the Sahel, Savanna and tropical Atlantic. The zonal flux of dust originating from the Bodélé indicates a strong seasonal dependences to Bodélé dust mobilisation activity and wind regime determining transport direction (see Fig. 7 and Table 2). In winter, dust export from the Bodélé occurs at lower tropospheric levels near the surface, peaking around 13° N (−3 Mg/month) at 10° W and around 18° N (−0.1 Mg/month) at 20° W. The Bodélé dust export is positive in summer at lower tropospheric heights (maximum export of 0.02 Mg/month at 10° W) and negative in the middle and upper troposphere (maximum backward transport of 4 kg/month at 10° W). In summer, dust export from the Bodélé is significantly lower than in winter, and additionally the dust layer originating from the Bodélé is mixed upward during transport towards the Atlantic. In summer, the WAM is dominant in the lower troposphere and transports air masses towards the Sahran heat low situated over the Western Sahara. Consequently a positive, eastward transport of dust occurs at low levels. Considering Bodélé dust alone, westward dust export fluxes seem to be in disagreement with the Saharan dust export including the Bodélé. The export of

Bodélé dust can be larger than the Saharan export as it includes westward (negative) and eastward (positive) fluxes as well as the vertical total flux can show different directions. Depending on leading wind regimes, total dust export can be positive for dust from the entire Sahara and Sahel domain but at the same time negative regarding the part of the dust originating from the Bodélé. However, mineral dust from the Bodélé Depression is able to reach higher tropospheric levels (Fig. 7) which is a precondition for long distance transport as crossing the Atlantic. For transport to South America, two preconditions are fulfilled during winter: wind regimes over the tropical Atlantic have a southwest component and the Bodélé is most active during this season.

3.6 Relationship of AOT, dust column load and deposition

In Sect. 3.4 the dust flux from North Africa towards the tropical and subtropical Atlantic is described using the regional dust emission and transport model LM-MUSCAT. Kaufman et al. (2005) propose a method to determine dust concentrations as well as dust fluxes and dust deposition from space-borne measurements. The authors used AOT based on MODIS (Moderate Resolution Imaging Spectroradiometer) observations to derive dust column concentrations assuming a constant ratio between atmospheric column dust load M_{dust} and AOT τ_{dust}:

$$\frac{M_{\mathrm{dust}}}{\tau_{\mathrm{dust}}} = 1.33\rho\,\frac{R_{\mathrm{eff}}}{Q} = 2.7 \pm 0.4\ \mathrm{g/m^2}, \tag{8}$$

with the density of dust particle ρ, the effective radius of dust particle R_{eff} and the light extinction efficiency Q. Results from the regional model LM-MUSCAT show a lower $M_{\mathrm{dust}}/\tau_{\mathrm{dust}}$-ratio of 1 g/m^2 (Fig. 9) instead of 2.7 g/m^2 assumed by Kaufman et al. (2005). No differences in this ratio pointing towards a seasonal or regional dependence can be found for the three simulated months. Kaufman et al. (2005) derive the AOT from the satellite measured radiance by using look-up tables for fine-mode aerosol (0.1 μm$\leq R_{\mathrm{eff}} \leq$0.25 μm) and coarse-mode aerosol (1 μm$\leq R_{\mathrm{eff}} \leq$2.5 μm). Differences for the $M_{\mathrm{dust}}/\tau_{\mathrm{dust}}$-ratio derived from LM-MUSCAT model results using five independent size bins (radius limits at: 0.1 μm, 0.3 μm, 0.9 μm, 2.6 μm, 8 μm and 24 μm) and the ratio proposed by Kaufman et al. (2005) might be influenced by different size distributions of the atmospheric dust load. This size distribution of dust computed by LM-MUSCAT have been compared with near source measurements (Heinold et al. 2008[4]), yielding good agreement. Measurement campaigns situated in far-source areas like the SAMUM-II and SOPRAN field measurements on the Cape Verde Islands will help to improve estimates of the dust size distribution and derived products as the AOT. Furthermore Kaufman et al. (2005) determine northern Atlantic dust deposition fluxes by assuming that the gradient of AOT between two points is related to the atmospheric removal of dust. To test, whether the derivation of mass fluxes from dust column concentrations based on AOT values is realistic, we compute dust fluxes through a meridional transect along 10° W and 20° W using three different approaches: dust flux computed using Eq. (7) at each level (case 1), using Eq. (7) but using total dust column concentration and zonal wind speed at a fixed height (800 hPa in winter, 700 hPa in summer) as in Kaufman et al. (2005) representing the transport height (case 2), and as case 2 but the total dust concentration derived from modelled AOTs following Eq. (6) and using a $M_{\text{dust}}/\tau_{\text{dust}}$-ratio of 2.7 g/m^2 (case 3). Comparing to dust fluxes computed directly from dust concentrations at each height level, large differences concerning the transported dust amount can be found for case 1 and 2. The dust load, normally inhomogeneously vertical distributed is assumed to be concentrated within the transport layer which leads to a lager dust export. The zonal wind speed reverses at a level of 1–2 km, where the direction of the wind changes due to the cell structure of the Hadley circulation. In case of fixed transport levels (case 2 and 3), the dust fluxes are less realistic due to resulting eastward dust fluxes than in case 1. However, by using zonal wind speeds the meridional component of the dust flux is not considered. Thus the gradient of dust fluxes result in higher dust deposition than directly compared due to not taking meridional dust transport as well as vertical diffusion into account. Dust fluxes for case 1 and case 2 are of similar magnitude. Differences are due to the layer-wise computation in case 1 taking the inhomogeneous vertical distribution of dust

ACPD
8, 16061–16096, 2008

concentration and wind in account, and the idealised vertical dust distribution by assuming a well defined transport layer at a fixed layer in case 2. Dust fluxes computed for case 2 and case 3 differ in the difference in factor of 2.7, reflecting the assumed M_{dust}/τ_{dust}-ratio following Kaufman et al. (2005) compared to the model results. Large deviations between the estimates exist for the summer months. For other seasons it can be expected that deposition fluxes derived from satellite retrieved AOT distributions yield satisfactory results, if the dust size distribution can be well characterised.

4 Conclusions

The study on Saharan dust export towards the North Atlantic presented here uses results of the regional model system LM-MUSCAT to describe seasonal characteristics of horizontal and vertical dust distributions and their evolution exemplarily for three case studies each covering a one-month period in different seasons. Transport of Saharan dust is characterised by the vertical and horizontal distribution of atmospheric dust concentrations, dry and wet deposition, and zonal dust fluxes. As airborne dust is an aerosol affected by meteorological features like wind, rain and turbulence changing with seasons, emission, transport, and deposition show seasonal characteristics.

Summer and winter are the most dissimilar seasons with regard to Saharan dust transport. In winter, dust concentration has its maximum in near-surface layers over the tropical latitudes. In summer, dust is transported above the trade winds inversion with a maximum westward transport at the lower subtropic latitudes. The vertical distribution of the zonal dust export clearly shows the relation of meridional dust export with general circulation pattern that is mainly controlled by the Hadley circulation. Considering the dust source activity controlling the atmospheric dust concentration, the Bodélé is most active during winter. Consequently the contribution of Bodélé dust to the Saharan dust load is maximum in winter months. Preconditions for long-range transport towards the South American rain forest are the best during winter months. The ratio of AOTs and deposition rates depends strongly on the height of the dust layer. The relation of dust deposition and AOT is evident for dust transported within the near-surface levels dust deposition is directly related to dust deposition, but this is not the case for elevated dust layers. In general, dust deposition rates cannot be derived directly from AOT measurements.

Zonal dust fluxes have been computed using three different approaches by taking the vertical inhomogeneity of the distribution of dust concentration and wind velocity into account. Gradients of dust fluxes between 10° W and 20° W have been compared to modelled deposition rates pointing towards the role of meridional dust transport especially in case of strong dust plumes, and the transport height.

Regional models provide a comprehensive data set in horizontal and vertical resolution and are able to capture local-scale features. Model deficiencies are evident for July 2006 for which modelled dust optical thicknesses are too low compared to MODIS retrievals, and the temporal evolution of dust AOT at the Cape Verde location was not matched well with AERONET sun-photometer measurements – although at this location the magnitude of AOT between measurements and model results agree in general. The results for this month indicate a possible overestimation of wet deposition of dust. Too low dust AOT indicates that the modelling of moist convective events which are relevant for dust mobilising processes in this region is deficient. Consequently detailed investigations on dust emission during meteorological summer conditions are required.

Acknowledgements. We thank the Deutscher Wetterdienst (DWD) for good cooperation and support. We also thank D. Tanré for his effort in establishing and maintaining AERONET Cabo Verde site. MODIS analyses used in this paper were produced with the Giovanni online data system, developed and maintained by the NASA Goddard Earth Sciences (GES) Data and Information Services Center (DISC).

References

Banta, R. M., Pichugina, Y. L., and Brewer, W.: Turbulent velocity-variance profiles in the stable Boundary Layer generated by a nocturnal low-level jet, J. Atmos. Sci., 63, 2700–2719, 2006.

16068
Barkan, J., Kutiel, H., Alpert, P., and Kishcha, P.: Synoptics of dust intrusion days from the African continent into the Atlantic Ocean, J. Geophys. Res., 109, D08201, doi:10.1029/2003JD004416, 2004. 16069
Berge, E.: Transboundary air pollution in Europe, MSC-W Status Rep. 1997, Part 1 and 2, EMEP/MSC-W Rep. 1/97, Norwegian Meteorol. Inst. Oslo, Norway, 1997. 16065
Blackadar, A. K.: Boundary Layer wind maxima and their significance for the growth of Nocturnal Inversion, B. Am. Meteorol. Soc., 38, 283–290, 1957. 16068
Chiapello, I., Bergametti, G., Gomes, L., Chatenet, B., Dulac, F., Pimenta, J., and Suares, E. S.: An additional low layer transport of Sahelian and Saharan dust over the North-Eastern Tropical Atlantic, Geophys. Res. Lett., 22, 3191–3194, 1995. 16070
Chiapello, I., Bergametti, G., Chatenet, B., Bousquet, P., Dulac, F., and Soares, E. S.: Origins of African dust transported over the northeastern tropical Atlantic, J. Geophys. Res., 102, 13 701–13 709, 1997. 16069, 16070
Doms, G. and Schättler, U.: A Description of the Nonhydrostatic Regional Model LM, Tech. Rep. Part I: Scientific Documentation, Deutscher Wetterdienst, Geschäftsbereich Forschung und Entwicklung, available at http://www.cosmo-model.org, 2002. 16064
Dunion, J. P. and Velden, C. S.: The Impact of the Saharan Air Layer on Atlantic Tropical Cyclone Activity, B. Am. Meterol. Soc., 353–365, 2004. 16069
Fung, I., Meyn, S., Tegen, I., Doney, S. C., John, J., and Bishop, J. K. B.: Iron supply and demond in the upper ocean, Global Biogeochem. Cy., 14, 281–296, 2000. 16063
Gao, Y., Kaufman, Y. J., Tanré, D., Kolber, D., and Falkowski, P. G.: Seasonal Distribution of Aeolian Iron Fluxes to the Global Ocean, Geophys. Res. Lett., 28, 29–32, 2001. 16063
Garratt, J. R.: The atmospheric boundary layer, Cambridge University Press, 334 pp., 1992. 16068
Goudie, A. S. and Middleton, N. J.: Saharan dust storms: nature and consequences, Earth-Sci. Rev., 56, 179–204, 2001. 16062
Heinold, B., Helmert, J., Hellmuth, O., Wolke, R., Ansmann, A., Marticorena, B., Laurent, B., and Tegen, I.: Regional Modeling of Saharan Dust Events using LM-MUSCAT: Model Description and Case Studies, J. Geophys. Res., 112, D11204, doi:10.1029/2006JD007443, 2007. 16064
Iversen, J. D. and White, B. R.: Saltation threshold on Earth, Mars and Venus, Sedimentology, 29, 111–119, 1982. 16064

ACPD
8, 16061–16096, 2008

Jacobson, H. A., Jonson, J. E., and Berge, E.: The multi-layer Eulerian model: Model description and evaluation of transboundary fluxes of sulphur and nitrogen species for one year, EMEP/MSC-W Note 2/97, Norwegian Meteorol. Inst., Oslo, Norway, 1997. 16065

Jickells, T. D., An, Z. S., Andersen, K. K., Baker, A. R., Bergametti, G., Brooks, N., Cao, J. J., Boyd, P. W., Duce, R. A., Hunter, K. A., Kawahata, H., Kubilay, N., LaRoche, J., Liss, P. S., Mahowald, N., Prospero, J. M., Ridgwell, A. J., Tegen, I., and Torres, R.: Global Iron Connections Between Desert Dust, Ocean Biogeochemistry, and Climate, Science, 308, 67–71, 2005. 16063

Journet, E., Desboeufs, K. V., Caquineau, S., and Colin, J.-L.: Mineralogy as a critical factor of dust iron solubility, Geophys. Res. Lett., 35, L07805, doi:10.1029/2007GL031589, 2008. 16062

Kalu, A. E.: The African dust plume: Its characteristics and propagation across west Africa in winter, SCOPE, 14, 95–118, 1979. 16067, 16068, 16069, 16088

Kaufman, Y. J., Koren, I., Remer, L. A., Tanré, D., Ginoux, P., and Fan, S.: Dust transport and deposition observed from the Terra-Moderate Resolution Imaging Spectroradiometer (MODIS) spacecraft over the Atlantic Ocean, J. Geophys. Res., 110, D10S12, 2005. 16063, 16074, 16077, 16078, 16079, 16087

Koren, I., Kaufman, Y., Washington, R., Todd, M. C., Rudich, Y., Martins, J. V., and Rosenfeld, D.: The Bodélé depression: a single spot in the Sahara that provides most of the mineral dust to the Amazon forest, Environ. Res. Lett., 1, 014005, doi:10.1088/1748-9326/1/1/014005, 2006. 16063, 16076

Lenschow, D. H. and Stankov, B.: The Rapid Morning Boundary-Layer Transition, J. Atmos. Sci., 36, 2108–2124, 1979. 16068

Luo, C., Mahowald, N., and del Corral, J.: Sensitivity study of meteorological parameters on mineral aerosol mobilization, transport, and distribution, J. Geophys. Res., 108, 4447, doi:10.1029/2003JD003483, 2003. 16062

Mahowald, N. M., Baker, A. R., Bergametti, G., Brooks, N., Duce, R. A., Jickells, T. D., Kubilay, N., Prospero, J. M., and Tegen, I.: Atmospheric global dust cycle and iron inputs to the ocean, Global Biogeochem. Cy., 19, GB4025, doi:10.1029/2004GB002402, 2005. 16062, 16063

Marticorena, B. and Bergametti, G.: Modeling the atmospheric dust cycle: 1. Design of a soil-derived dust emission scheme, J. Geophys. Res., 100, 16 415–16 430, 1995. 16064

Middleton, N. J. and Goudie, A. S.: Saharan dust: sources and trajectories, Trans. Inst. Br.

Geogr., 26, 165–181, 2001. 16062
Moore, C. M., Mills, M. M., Milne, A., Langlois, R., Achterberg, E. P., Lochte, K., Geider, R. J., and Roche, J. L.: Iron limits primary productivity during spring bloom development in the central North Atlantic, Glob. Change Biol., 12, 626–634, doi:10.1111/j.1365-2486.2006.01122.x, 2006. 16063
Nappo, C. J.: Sporadic Breakdowns of Stability in the PBL over Simple and Complex Terrain, Bound.-Lay. Meterol., 54, 69–87, 1991. 16068
Neuer, S., Torres-Padrón, M. E., Gelado-Caballero, M. D., Rueda, M. J., Hernández-Brito, J., Davenport, R., and Wefer, G.: Dust deposition pulses to the eastern subtropical North Atlantic gyre: Does ocean's biogeochemistry respond?, Global Biogeochem. Cy., 18, GB4020, doi:10.1029/2004GB00228, 2004. 16063
Parker, D. J., Burton, R. R., Diongue-Niang, A., Ellis, R. J., Felton, M., Taylor, C. M., Thorncroft, C. D., Bessemoulin, P., and Tompkins, A. M.: Thei diurnal cycle of the West African monsoon circulation, Q. J. Roy. Meteor. Soc., 131, 2839–2860, doi:10.1256/qj.04.52, 2005. 16068
Prospero, J. M., Glaccum, R. A., and Nees, R. T.: Atmospheric transport of soil dust from Africa to South America, Nature, 289, 570–572, 1981. 16070
Prospero, J. M., Ginoux, P., Torres, O., Nicholson, S. E., and Gill, T. E.: Environmental characterization of global sources of atmospheric soil dust identified with the Nimbus 7 Total Ozone Mapping Spectrometer (TOMS) absorbing aerosol product, Rev. Geophys., 40, 1002, doi:10.1029/2000RG000095, 2002. 16062, 16075
Romero, O. E., Lange, C. B., Swap, R., and Wefer, G.: Eolian-transported freshwater diatoms and phytoliths across the equatorial Atlantic: Temporal changes in Saharan dust transport patterns, J. Geophys. Res., 104, 3211–3222, 1999. 16062
Sarthou, G., Baker, A. R., Blain, S., Achterberg, E. P., Boye, M., Bowie, A. R., Croot, P., Laan, P., de Baar, H. J. W., Jickells, T. D., and Worsfold, P. J.: Atmospheric iron deposition and sea-surface dissolved iron concentrations in the eastern Atlantic Ocean, Deep-Sea Res. Part I, 50, 1339–1352, doi:10.1016/S0967-0637(03)00126-2, 2003. 16063
Sarthou, G., Baker, A. R., Kramer, J., Laan, P., Laës, A., Ussher, S., Achterberg, E. P., de Baar, J. H. W., Timmermans, K. R., and Blain, S.: Influence of atmospheric inputs on the iron distribution in the subtropical North-East Atlantic Ocean, Mar. Chem., 104, 186–202, doi:10.106/j.marchem.2006.11.004, 2007. 16063
Schepanski, K., Tegen, I., Laurent, B., Heinold, B., and Macke, A.: A new Saharan dust source activation frequency map derived from MSG-SEVIRI IR-channels, Geophys. Res. Lett., 34,

L18803, doi:10.1029/2007GL030168, 2007. 16066

Tegen, I., Harrison, S. P., Kohfeld, K., and Prentice, I. C.: Impact of vegetation and preferential source areas on global dust aerosol: Results from a model study, J. Geophys. Res., 107, 4576, doi:10.1029/2001JD000963, 2002. 16064

Tiedtke, M.: A comprehensive mass flux scheme for cumulus parameterisation in large-scale models, Mon. Weather Rev., 117, 1779–1799, 1989. 16064

Tsyro, S. and Erdman, L.: Parameterisation of aerosol deposition processes in EMEP MSC-E and MSC-W transport models, EMEP/MSC-W Note 7/00, Norwegian Meteorol. Inst., Oslo, Norway, 2000. 16065

Washington, R. and Todd, M. C.: Atmospheric contronls on mineral dust emission from the Bodélé Depression, Chad: The role of the low level jet, Geophys. Res. Lett., 32, L17701, doi:10.1029/2005GL023597, 2005. 16076

Washington, R., Todd, M., Middleton, N. J., and Goudie, A. S.: Dust-Storm Source Areas Determined by the Total Ozone Monitoring Spectrometer and Surface Observations, Ann. Assoc. Am. Geogr., 93, 297–313, 2003. 16062, 16066, 16075

Wedepohl, K. H.: The composition of the continental crust, Geochim. Cosmochim. Ac., 59, 1217–1232, 1995. 16062

Wolke, R., Hellmuth, O., Knoth, O., Schröder, W., Heinrich, B., and Renner, E.: The chemistry-transport modeling system LM-MUSCAT: Description and CityDelta applications, in: Air Polution Modeling and Its Aplication XVI, edited by: Borrego, C. and Incecik, S., Proceedings of twenty-sixth NATO/CCMS international technical meeting on air polution modeling and its application, 427–437, 2004a. 16064

Wolke, R., Hellmuth, O., Knoth, O., Schröder, W., and Renner, E.: The parallel model system LM-MUSCAT for chemistry-transport simulations: Coupling scheme, parallelization and application, Parallel Computing: Software Technology, Algorithms, Architectures, and Applications, 363–370, 2004b. 16064

Zender, C. S. and Newman, D.: Spatial heterogeneity in aeolian erodibility: Uniform, topographic, geomorphic, and hydrologic hypotheses, J. Geophys. Res., 108, 4543, doi:10.1029/2002JD003039, 2003. 16063

Table 1. Zonal Saharan dust export (Tg/month) through a meridional transect at 10° W and 20° W. Monthly sums are derived from hourly dust export computations at each model layer.

January 2007	10° W	15° W	20° W
2.5–10° N	−2.5	−0.7	−0.02
10–20° N	−2.1	−1.1	−1.5
20–30° N	−0.7	−1.3	0.8
30–40° N	0.2	0.3	0.5
July 2006	**10° W**	**15° W**	**20° W**
2.5–10° N	−0.8	−0.7	−3.5
10–20° N	−0.9	−0.7	−3.5
20–30° N	−0.5	−0.04	0.4
30–40° N	2.0	1.5	3.5

ACPD

8, 16061–16096, 2008

Seasonal Saharan dust transport and deposition

K. Schepanski et al.

ACPD
8, 16061–16096, 2008

Seasonal Saharan dust transport and deposition

K. Schepanski et al.

Table 2. Zonal dust export from the Bodélé (Tg/month) through a meridional transect at 10° W and 20° W. Monthly sums are derived from hourly dust export computations at each model layer.

January 2007	10° W	15°	20° W
2.5–10° N	−2.0	−0.01	0.01
10–20° N	−8.2	−1.1	0.8
20–30° N	0.5	0.4	0.4
30–40° N	0.08	0.1	0.2
July 2006	**10° W**	**15°**	**20° W**
2.5–10° N	−0.06	−0.05	−0.04
10–20° N	−0.1	−0.1	0.005
20–30° N	−0.001	0.06	0.003
30–40° N	0.002	0.03	0.003

Table 3. Zonal Saharan dust export (Tg/month) through a meridional transect at 10° W and 20° W, starting at 2.5° N and ending at 40° N. Deposition rates (Tg/month) for the area defined by the transects are derived from either modelled deposition rates or from gradients of concentration between the transects. To compute dust export, three different approaches have been used: (case 1) export computed using dust concentration and wind at each model layer, (case 2) export computed using modelled dust concentrations but assuming a well-defined dust layer at 800 hPa in winter and 700 hPa in summer, fluxes computed with winds at these layers, and (case 3) export computed using modelled AOT concentrations, after Kaufman et al. (2005).

	case 1		case 2		case 3		case 1	case 2	case 3	
Month	10° W	20° W	10° W	20° W	10° W	20° W	ΔM	Δ M	ΔM	deposition
January 2007	−5.1	−0.2	−6.1	−1.4	−17	−3.7	−4.9	−4.7	−13	3.1
March 2006	0.9	5.1	−0.2	3.6	−0.5	9.8	−4.2	−3.8	−10	4.0
July 2006	−0.2	−3.1	−0.7	0.1	−1.9	0.4	2.9	−0.8	−2.3	0.6

ACPD

8, 16061–16096, 2008

Seasonal Saharan dust transport and deposition

K. Schepanski et al.

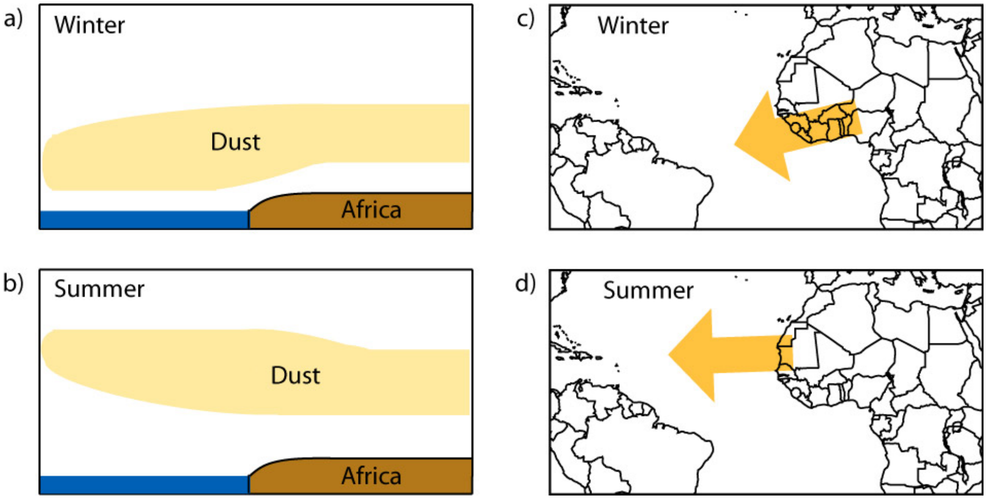

Fig. 1. Schematic diagram of vertical and horizontal dust export from North Africa towards the tropical East Atlantic for winter **(a, c)** and summer **(b, d)**. Schematics following Kalu (1979).

ACPD
8, 16061–16096, 2008

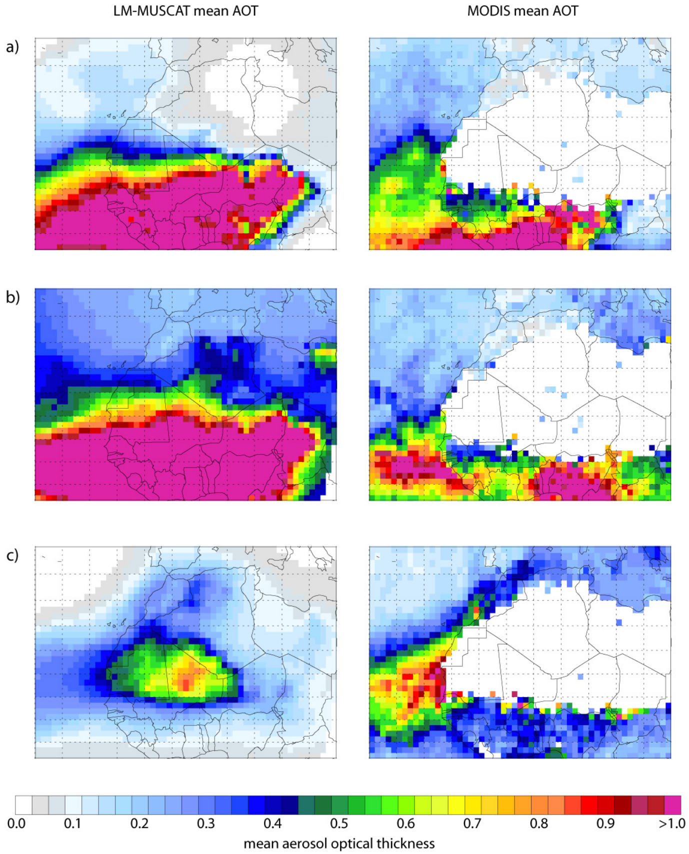

Fig. 2. Monthly mean AOT for January 2007 **(a)**, March 2006 **(b)** and July 2006 **(c)** from results of regional modelling and MODIS measurements. The satellite data are provided freely by GIOVANNI MODIS Online Visualization and Analysis System (MOVAS) (http://g0dup05u.ecs.nasa.gov/Giovanni/).

ACPD

8, 16061–16096, 2008

Seasonal Saharan dust transport and deposition

K. Schepanski et al.

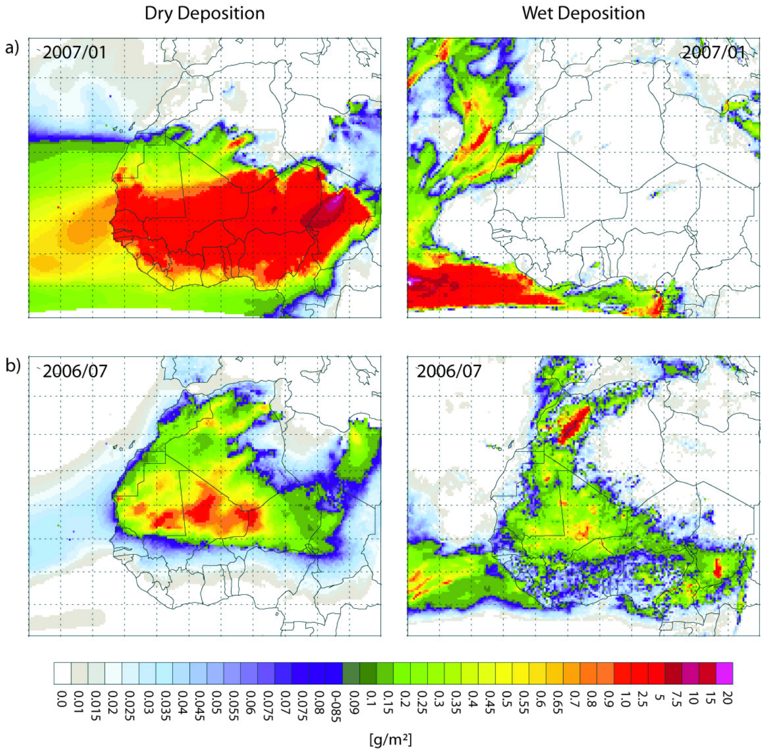

Fig. 3. Monthly dust dry and wet deposition fluxes for January 2007 **(a)** and July 2006 **(b)**, computed by the regional model LM-MUSCAT.

ACPD
8, 16061–16096, 2008

Seasonal Saharan dust transport and deposition

K. Schepanski et al.

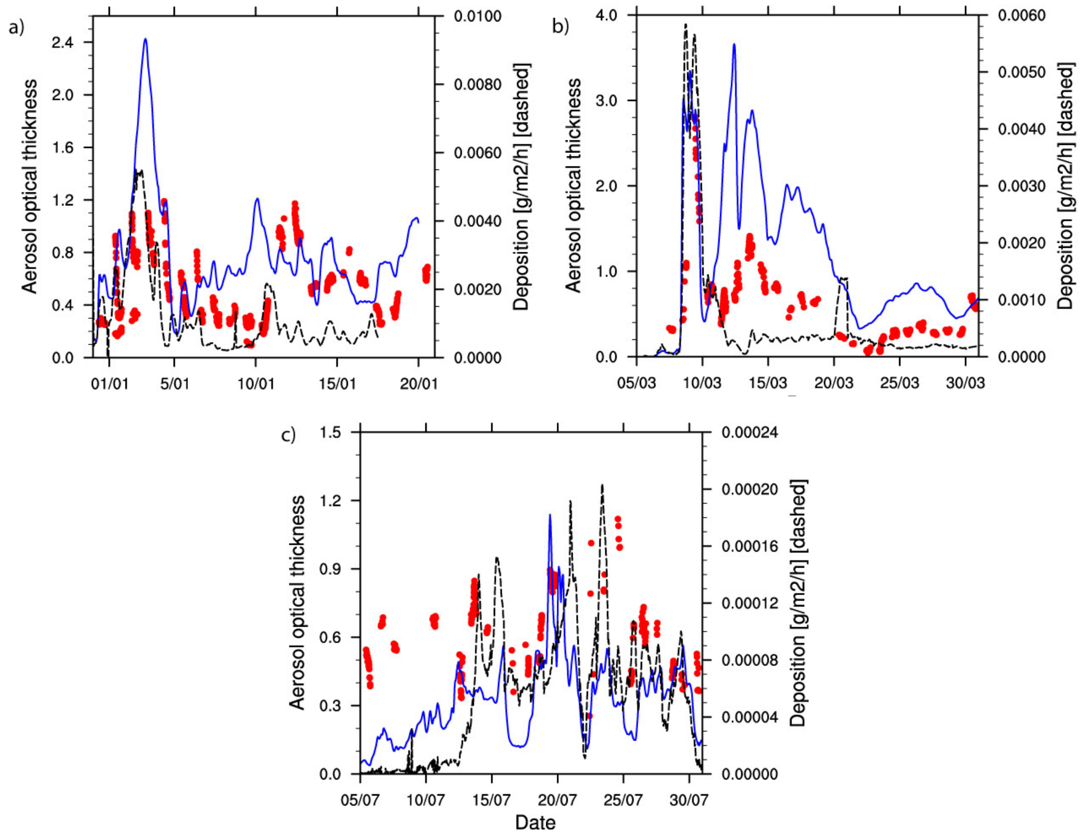

Fig. 4. Modelled (blue solid line) and observed AOT (red solid dots) over Sal, Cape Verde (16° N; 22° W) for January 2007 **(a)**, March 2006 **(b)** and July 2006 **(c)** and modelled dust deposition (black dashed line). Observations are provided by AERONET, http://aeronet.gsfc.nasa.gov.

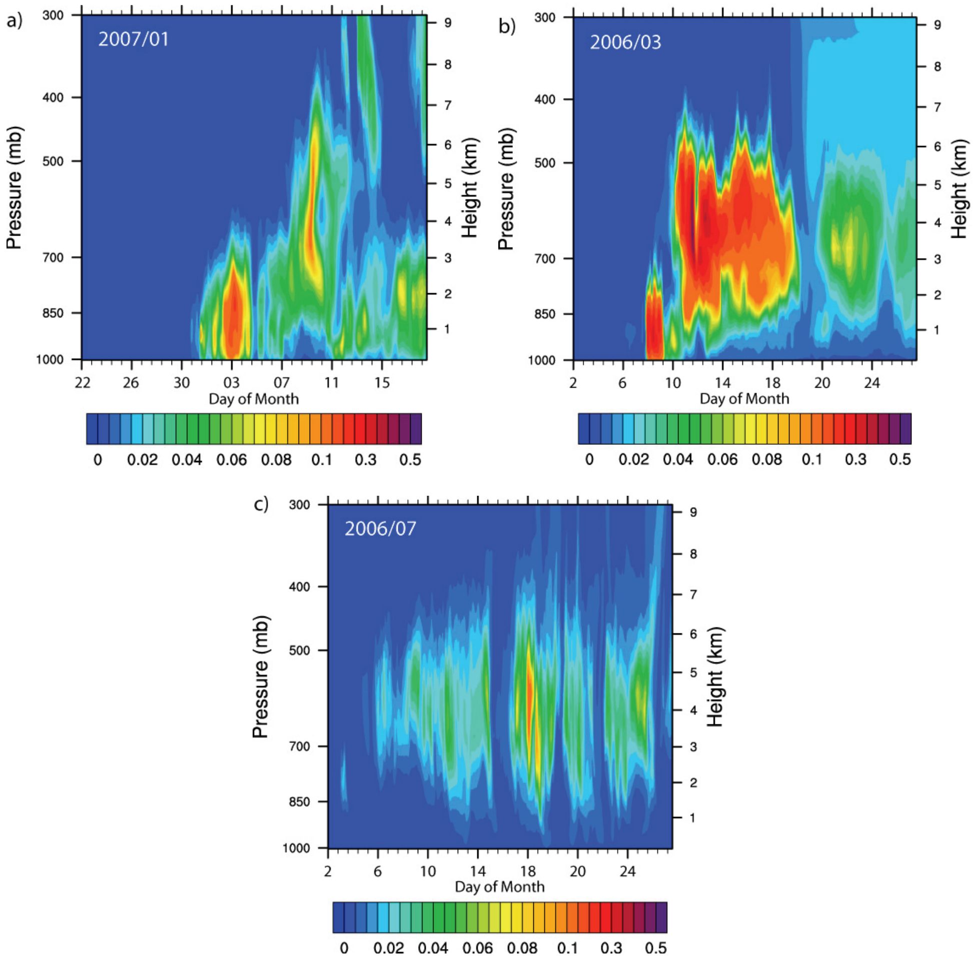

Fig. 5. Temporal evolution of the vertical dust concentration (g/m^2) distribution over Sal, Cape Verde (16° N; 22° W) for January 2007 **(a)**, March 2006 **(b)** and July 2006 **(c)**.

ACPD

8, 16061–16096, 2008

Seasonal Saharan dust transport and deposition

K. Schepanski et al.

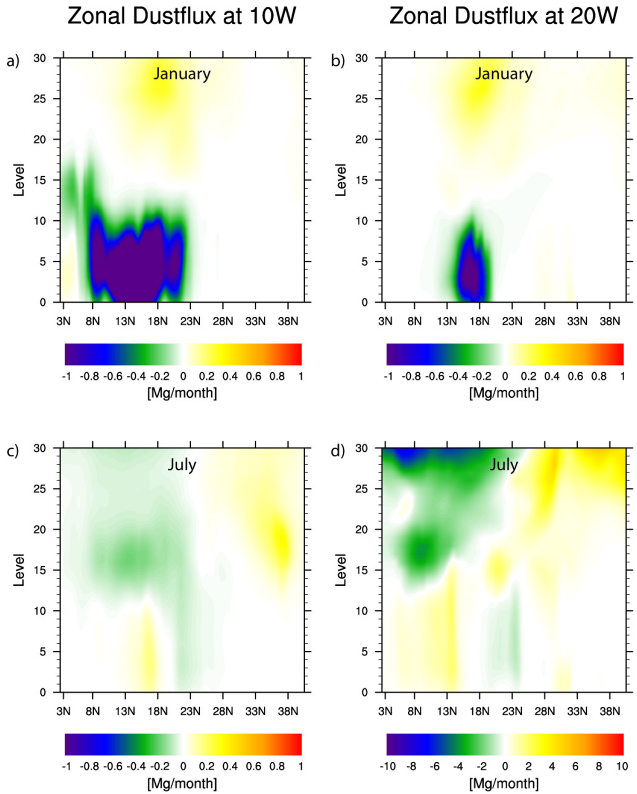

Fig. 6. Vertical distribution of the monthly zonal dust transport towards 10° W and 20° W for winter (January 2007) and summer (July 2006). Eastward fluxes are positive, westward fluxes are negative corresponding to the common definition of wind vectors.

ACPD
8, 16061–16096, 2008

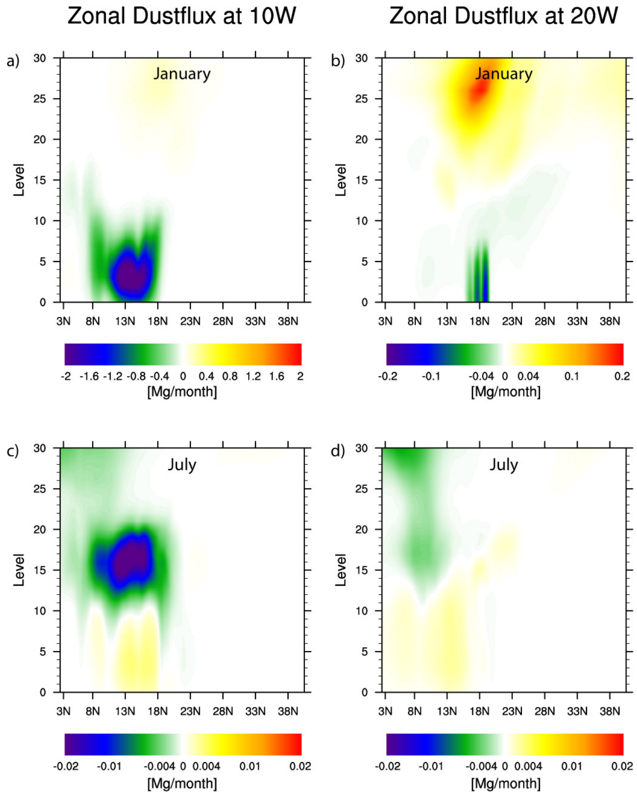

Fig. 7. Vertical distribution of the monthly zonal transport of dust originating from the Bodélé Depression towards 10° W and 20° W for winter (January 2007) and summer (July 2006). Eastward fluxes are positive, westward fluxes are negative corresponding to the common definition of wind vectors.

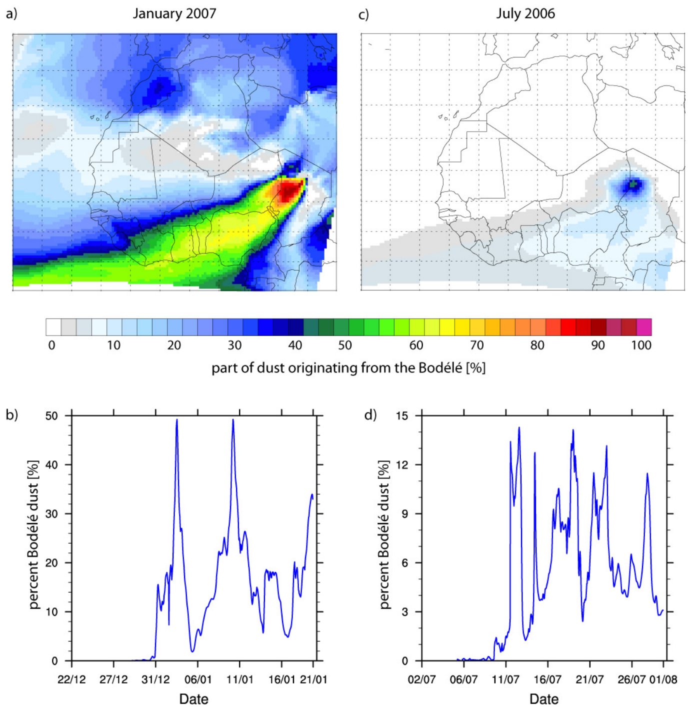

Fig. 8. Percentage of dust concentration originating from the Bodélé Depression source region compared to total dust. **(a)** and **(c)** show the horizontal distribution of the contribution of Bodélé, **(b)** and **(d)** the part of Bodélé dust over the Cape Verde Islands (16° N; 22° W). (a) and (b) winter (January 2007), (c) and (d) summer (July 2006).

ACPD
8, 16061–16096, 2008

Seasonal Saharan dust transport and deposition

K. Schepanski et al.

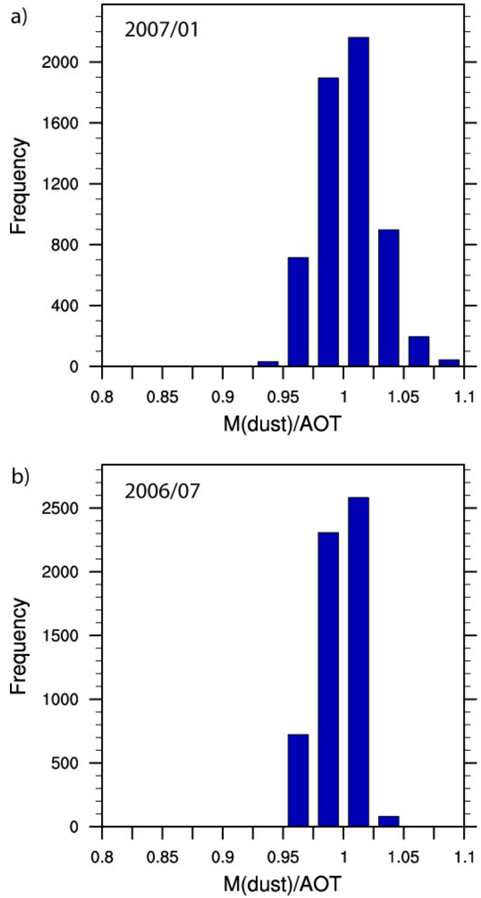

Fig. 9. Frequency distribution of ratio of column dust concentration and AOT for **(a)** January 2007, **(b)** March 2006 and **(c)** July 2006 following a transect at 16.7° N from 30° W west of the Cape Verde Archipelago to 20° E east of the Bodélé Depression.

ACPD
8, 16061–16096, 2008